EUROPEAN FUSION DEVELOPMENT AGREEMENT

EFDA–JET–PR(04)18

G. Tresset, X. Litaudon, D. Moreau, X. Garbet and JET EFDA contributors

A Dimensionless Criterion for Characterizing Internal Transport Barriers in JET

A Dimensionless Criterion for Characterizing Internal Transport Barriers in JET

G. Tresset, X. Litaudon, D. Moreau, X. Garbet and JET EFDA contributors*

DRFC, Association Euratom–CEA, CEA Cadarache, Saint-Paul-lez-Durance, France
** See annex of J. Pamela et al, "Overview of Recent JET Results and Future Perspectives", Fusion Energy 2002 (Proc. 19th IAEAFusion Energy Conference, Lyon (2002)).*

Preprint of Paper to be submitted for publication in
Nuclear Fusion

ABSTRACT

Analysis of experiments performed at different heating powers and magnetic field intensities shows that the existence of internal transport barriers in JET can be inferred in regions of space–time where the ratio of the ion gyroradius to the local gradient scale length exceeds some critical value. A possible interpretation leading to the theoretical relevance of this dimensionless parameter as a local indicator of a bifurcated plasma state is the stabilization of turbulence by the $\boldsymbol{E} \times \boldsymbol{B}$ shear flows associated with large pressure gradients and plasma rotation. Large database analysis and real time plasma control are envisaged as attractive applications.

1. INTRODUCTION

Several recent experiments realized in various tokamaks have demonstrated the existence of high performance regimes in which a so-called internal transport barrier (ITB) appears [1]. An ITB is defined as a plasma region where anomalous transport is eliminated or strongly reduced, and, because of the important role of the local magnetic and flow shears in the emergence of such barriers, discharges with ITBs have been originally referred to on JET as the 'optimized shear' (OS) discharges. Analysis of experiments performed at various magnetic field intensities has pointed to an apparent magnetic field dependent power threshold for the emergence of ITBs in regions of weak positive magnetic shear [2]. This observation motivated our search for an objective and more physical existence criterion incorporating this dependence, but expressed in terms of some dimensionless parameters. This could possibly lead to a better understanding and quantification of the physical processes leading to the formation of ITBs, and to the emergence of appropriate scaling laws for advanced tokamak regimes.

Another motivation for an objective characterization of ITBs stems from practical considerations. Analyses of the JET experimental database frequently require the identification of some typical ITB features such as the onset time, location, collapse time and dynamics of the barrier. An intuitive method often employed so far is to locate a visible 'break' on the temperature profiles or, alternatively, one can resort to the computation of the thermal diffusivity profiles and look for a region of reduced transport.

These somewhat subjective and rather cumbersome procedures for assessing the existence and location of ITBs are not efficient for an extensive database study, and are inadequate for an active control of their evolution as was proposed for instance in ref. [3]. Microturbulence and transport theories of tokamak plasmas could provide an alternative, but they are complicated and usually require large numerical codes for an accurate quantitative analysis, at a high computational cost. Applying turbulence stabilization criteria from first principles theories is therefore not suitable either for an efficient assessment of ITB formation in analysing large sets of discharges or for real time control applications. Hence, there is a real interest in following a more pragmatic approach and developing some physical but practical criterion which could be used routinely to speed up the identification of ITBs, to characterize their main features and possibly to control their dynamics.

Dimensional analysis is probably the best guideline for selecting the appropriate variables for such an approach. It indeed provides a bridge between the statistical observations made in some specific experiments and the relevant ingredients of a more general theory, and it also provides a framework for further research involving broader sets of experiments and multimachine comparisons. Thus, even though our criterion may not be as universal as a genuine first principles criterion could be—owing to the specificity of the JET experiments under consideration and to the semiempirical nature of the analysis—its expression in terms of appropriate dimensionless variables should be more closely related to the underlying physics than, for instance, a power threshold in megawatts or a dependence upon engineering variables such as the magnetic field intensity in teslas.

A local ITB criterion serving these purposes is proposed in this article. In section 2, we first describe this criterion, showing how it naturally appears from the most basic and generic parameters of conventional theories. Then we discuss how the measurement uncertainties can be taken into account for a better assessment of the criterion fulfilment, and finally we show the statistical relevance of the proposed ITB criterion for the JET experimental OS database. In section 3 we suggest a possible theoretical interpretation of our findings by further developing a dimensional analysis which involves the main ingredients of microturbulence theory in magnetized plasmas. The concluding section is devoted to a summary with a brief discussion of the applicability of the proposed criterion and its generalization.

2. CRITERION FOR CHARACTERIZING THE EMERGENCE AND EVOLUTION OF ITBS

2.1. DIMENSIONLESS FORM OF THE CRITERION AND UNDERLYING PHYSICAL CONCEPTS

The physical mechanisms of barrier formation have not yet been completely identified, but drift waves are thought to make the principal contribution to microturbulence when the plasma is driven far from thermodynamic equilibrium, and drift wave stabilization is probably the cause of a transport reduction leading to the emergence of ITBs [4, 5]. Despite a variety of possible unstable modes, such as the ion temperature gradient (ITG) mode or the trapped electron modes (TEMs), a fundamental characteristic length arises from their dispersion relations: the ion Larmor radius at the sound speed, $\rho_s = c_s/\omega_{ci}$, where c_s is the ion sound speed and ω_{ci} the ion cyclotron frequency. Several studies have been carried out on various tokamaks to determine how the thermal diffusivities scale with respect to ρ_s (or, more exactly, with the normalized Larmor radius $\rho^* = \rho_s/a$, where a is the minor radius), and have given rise to the so-called 'Bohm' or 'gyro-Bohm' scalings [6]. When transport barriers appear, local gradient scale lengths become much shorter than the plasma size and, for a local analysis, one should indeed normalize the drift wave scale length ρ_s to the local temperature gradient scale length, for example $L_{Ti} = -T_i/(\partial T_i/\partial R)$ or $L_{Te} = -T_e/(\partial T_e/\partial R)$, where T_i (respectively, T_e) is the ion (respectively, electron) temperature and R is the plasma major radius on the equatorial plane. We therefore define the local dimensionless Larmor radius, ρ^*_T, as $\rho^*_T = \rho_s/L_T$ and consider either ρ^*_{Ti} or ρ^*_{Te}.

Clearly, for given toroidal magnetic field, ion species and plasma temperature, ITBs can be

characterized by values of the temperature or pressure gradients which are significantly larger than those of conventional L mode, or even H mode, discharges (discarding the edge temperature pedestal region). In such a case, i.e. when comparing discharges with the same global parameters, there are no differences in considering the absolute gradients, the associated characteristic length L_T or even the ratio of this length to the ion Larmor radius to characterize the emergence of an ITB. But when considering various experimental scenarios with different plasma currents and, more importantly, with a wide range of heating powers and magnetic field intensities, it is worth testing whether an ITB existence criterion could possibly be expressed according to the local value of ρ^*_T as it would intrinsically contain a strong magnetic field dependence. Noting that the simplest dimensionless criterion would be

$$\rho^*_T(R, t) \geq \rho^*_{ITB} \Leftrightarrow \text{an ITB exists at radius } R \text{ and time } t \tag{1}$$

the critical dimensionless number ρ^*_{ITB}, if it does exist, should depend on only a few dimensionless parameters and can in principle be evaluated experimentally by comparing discharges with and without ITBs and with different dimensional parameters such as toroidal magnetic field, heating powers, main ion species and plasma current.

2.2. EXPERIMENTAL UNCERTAINTIES AND CONFIDENCE FACTOR FOR THE FULFILMENT OF THE CRITERION

The measurements required for computing $\rho^*_T(R, t)$ are the electron and/or the ion temperature profiles, and the toroidal magnetic field which is taken on the magnetic axis. Unavoidably all these data are corrupted by uncertainties quantified by their associated standard deviations. Therefore the binary problem of deciding whether there is an ITB or not can also be answered in terms of a confidence factor for the criterion (1) to be fulfilled consistently with the measurement uncertainties. The electron temperature profiles were measured by an electron cyclotron emission (ECE) heterodyne radiometer which offers an excellent resolution (0.5ms/2cm) and an accuracy of about 5%, whereas the ion temperature profiles were obtained by charge exchange spectroscopy with a much lower resolution (50ms/10cm) and an accuracy of about 5%. The term $L^{-1}_T = -\partial \ln T/\partial R$ is computed as the logarithmic radial derivative of the temperature on the equatorial plane by applying a three point difference formula. The measurement uncertainties are combined with the standard propagation of errors to yield the relevant standard deviations for ρ^*_T, $\sigma_{\rho T^*}$. This calculation is performed as follows: let $X_1, \ldots, X_N$ be independent random variables whose standard deviations are $\sigma_{X1}, \ldots, \sigma_{XN}$ and let Y be another random variable defined by $Y = f(X_1, \ldots, X_N)$, where f is a regular function of N variables. Then, at first order, the standard deviation of Y, σ_Y, is given by

$$\sigma_Y^2 \approx \sum_{i=1}^{N} \left(\frac{\partial f}{\partial X_i}\right)^2 \sigma_{X_i}^2 \tag{2}$$

The unknown random variable here is the dimensionless Larmor radius ρ^*_T at the major radius

$R(k)$ as a function of $T_e(k)$, $T(k-1)$ and $T(k+1)$:

$$\begin{aligned}\rho_T^*(k) &= \rho_s(k)\,\frac{1}{L_T(k)} \\ &\approx \frac{1}{ZB_\phi}\sqrt{\frac{m_i}{e}}\sqrt{T_e(k)}\,\frac{1\mathrm{n}\,T(k-1)-1\mathrm{n}\,T(k+1)}{R(k+1)-R(k-1)}\end{aligned} \tag{3}$$

with Z the ion charge, B_ϕ the toroidal magnetic field, m_i the ion mass and e the electric charge. By taking the measurement uncertainties as the standard deviations $\sigma_{Te}(k)$, $\sigma_T(k-1)$ and $\sigma_T(k+1)$, the estimated error on $\rho^*_T(k)$ is then straightforward,

$$\begin{aligned}\sigma_{\rho_T^*}(k) \approx \frac{1}{ZB_\phi}\sqrt{\frac{m_i}{e}}\,&\frac{\sqrt{T_e(k)}}{|R(k+1)-R(k-1)|} \\ &\times\left[\frac{1}{4}\left(1\mathrm{n}\frac{T(k-1)}{T(k+1)}\right)^2\varepsilon_{T_e}^2+2\varepsilon_T^2\right]^{1/2}\end{aligned} \tag{4}$$

where ε_{Te} and ε_T stand for the relative uncertainties in the temperatures T_e and T (typically 5%).

Then, assuming a normal distribution,

$$p_{\rho_T^*,\sigma_{\rho_T^*}}(x) = \frac{1}{\sqrt{2\pi}\,\sigma_{\rho_T^*}}\exp\left(\frac{(x-\rho_T^*)^2}{T(k+1)}\right) \tag{5}$$

the probability that ρ^*_T exceeds the critical value is given by

$$\begin{aligned}\wp_{ITB}(R,t) &= \wp\left[\rho_T^*(R,t) \geqslant \rho_{ITB}^*\right] \\ &= \int_{\rho_{ITB}^*}^{+\infty} p_{\rho_T^*,\sigma_{\rho_T^*}}(x)\,dx.\end{aligned} \tag{6}$$

This figure of merit will be referred to as a confidence factor for identifying an ITB at a given time and radius.

2.3. EXPERIMENTAL VALIDATION OF THE PROPOSED ITB CRITERION

An attractive representation of the results is obtained by plotting contours of either ρ^*_T or $\wp_{ITB}$ in the (t, R) plane. The constant-ρ^*_T contours are plotted only for $\rho^*_T \geq \rho^*_{ITB}$ and the constant-$\wp_{ITB}$ contours are plotted only for $\wp_{ITB} \geq 50\%$ ($\wp_{ITB} = 50\%$ is obtained when the expectation value of ρ^*_T equals ρ^*_{ITB}). Figure 1(a) shows an example of such a graph for a discharge where the ITB dynamics is rich with events. The transport barrier is triggered in theLHCDprelude probably by a strongly negative magnetic shear and undergoes several short collapses due to core MHD activity. It can be seen that all the relevant information such as onset time, collapse times, as well as the expansion, contraction and width of the barrier, appear explicitly for a low computational cost. The dynamics and width given by the criterion are in good agreement with an analysis performed on the profiles (Fig.1(b)). The normalized radius, $\rho = (\Phi/\Phi_{max})^{1/2}$, with Φ the toroidal flux through a

poloidal section and Φ_{max} its maximum value has been used here instead of R to label flux surfaces.

The critical value ρ^*_{ITB} was chosen from a Pulse: with a perfectly visible barrier whose emergence time was well defined and which was used as a reference (Pulse No: 48993). It was thus found that $\rho^*_{ITB} \approx 1.4 \times 10^{-2}$ would match both the emergence time and the radial evolution of the barrier satisfactorily. Discharges obtained with almost the same operating conditions but which either exhibit an ITB or do not (as seen, for instance, from the neutron yield time traces) were also compared and successfully distinguished by the $\rho^*_T \geq 1.4 \times 10^{-2}$ criterion. ITBs observed on the ion temperature profile can also be detected according to ρ^*_T despite the smaller resolution of the T_i measurements (Fig.2). Quite interestingly, the same ρ^*_{ITB} value is again in good agreement with the information that can be independently gained from a detailed analysis of the discharges. Some plasmas, such as Pulse No: 49680, also exhibit a double internal barrier [7]. This double barrier was observed on the electron temperature (Fig. 3) and the ρ^*_T criterion was again in good agreement with the observations. It must be noted that ρ^*_{ITB} does not characterize the final state of the plasma but is to be understood as a critical value beyond which ρ^*_T goes when the plasma experiences a local transport bifurcation. This means that after a barrier has formed, ρ^*_T is not limited to ρ^*_{ITB}, and that various degrees of temperature gradient strengths and barrier widths develop, as also observed on other tokamaks.

In order to evaluate its reliability for detecting the presence and evolution of ITBs, our criterion was tested on many discharges from the JET OS database under various experimental conditions. For this purpose 116 deuterium discharges were selected with toroidal magnetic fields varying from 1.8 to 4T, plasma currents from 1.6 to 3.6MA (safety factors from 3.3 to 4.3), central densities from 2×10^{19} to 5.5×10^{19} m^{-3}, NBI power from 4.8 to 18.7MW and ICRH power from 0 to 8.7MW. Mainly electron temperature barriers are considered here because of the good spatial and temporal resolutions of the ECE diagnostic. Among these 116 Pulses, 84 have an ITB. Their emergence times were then independently evaluated by identifying a divergence between temperature traces from neighbouring radii and are compared with the ρ^*_T criterion in Fig.4(*a*). In addition, their emergence major radii given by the criterion were also compared with the radii at which a 'break' on the profiles can be seen as pictured in Fig.4(*b*). Only five very weak barriers were not detected by the criterion, whereas one detection was not really assessed by a detailed data analysis.

3. AN INTERPRETATION ON THE BASIS OF DIMENSIONAL ANALYSIS

A possible mechanism for the stabilization of the ITG modes and TEMs in tokamaks combines the $\boldsymbol{E} \times \boldsymbol{B}$ rotational flow and the magnetic shear effects, as has been found by several authors through the extensive use of computer codes [8–13]. The distortion of the convective cells by shear flow decreases the anomalous transport, and leads to a complete quench of the microturbulence when the shear rate is high enough. Nonlinear simulations of ITG modes showed that this occurs when the $\boldsymbol{E} \times \boldsymbol{B}$ shear rate γ_E exceeds the maximum linear growth rate of the local modes γ_{max} [9, 10]. A detailed analysis of our results in terms of such physical mechanisms would require local measurements of the plasma parameters—and of their gradients—with sufficient accuracy to

evaluate—γ_E and γ_{max} across the plasma radius and to compare their profiles. In JET, the radial electric field E_r could be evaluated from the various terms composing the fluid force balance equation for carbon impurities. This involves a spectroscopic measurement of the carbon pressure gradient and toroidal velocity, and a calculation of its poloidal velocity through neoclassical theory, i.e. through an accurate algebraic combination of the carbon density, temperature and pressure gradients. The $\boldsymbol{E} \times \boldsymbol{B}$ shear rate then involves the first radial derivative of all these terms [14]—including the second derivative of the pressure—and is therefore inaccurately determined. The same is true for the magnetic shear, which is an important ingredient in calculating the growth rates of the unstable modes, but involves the radial derivative of the safety factor profile *q(r)*. In addition, the motional Stark effect diagnostic was not operational for the discharges under consideration here and the *q* profiles were therefore poorly resolved. As a result, a direct local comparison of γ_{max} with γ_E did not allow any significant conclusions to be drawn as to whether $\gamma_E \approx \gamma_{max}$ at the times and radii where ITBs are formed, for the large set of discharges which are considered here.

A tentative interpretation of our results can, however, be sketched as follows and is worth developing. By resorting to dimensional analysis, i.e. by considering the orders of magnitude of the various terms at the locations where they are maximum and their respective scalings with respect to ρ^*_T, it is indeed possible, as shown below, to recast the stabilization criterion $\gamma_E \geq \gamma_{max}$ in the form $\rho^*_T \geq \rho^*_{ITB}$, thus pointing to the plausibility of the dimensionless parameter ρ^*_T being of theoretical relevance as a local indicator of plasma states with reduced turbulence.

From the force balance equation of the main ion species, the radial electric field in a tokamak is related to the ion pressure gradient and velocity through the relation

$$E_r = (Z_i e n_i)^{-1} (dp_i/dr) - V_{\theta i} B_{i\phi} + V_{\theta i} B_{\theta}. \tag{7}$$

Accordingly, the $\boldsymbol{E} \times \boldsymbol{B}$ shear rate can be decomposed into a 'diamagnetic part' $\gamma_{E,\,dia}$, a poloidal velocity contribution $\gamma_{E,\,\theta}$ and a toroidal velocity contribution $\gamma_{E,\,\phi}$. The link between $\boldsymbol{E} \times \boldsymbol{B}$ shear stabilization and a criterion of the form $\rho^*_T \geq \rho^*_{ITB}$ can be revealed by expressing frequencies in units of c_s/L_T and developing γ_E and γ_{max} in powers of ρ^*_T.

The growth rates of drift microinstabilities scale generically as c_s/L_T and can be written as

$$\gamma_{max} = (C_S/L_T) G_1 (\Lambda_T, s, q, \beta, \nu^*, \ldots) \tag{8}$$

where the function G_1 describes the stability of the most unstable mode. For the class of profiles at given β and collisionality ν^*, this function should depend mainly on the gradient length $\Lambda_T = L_T/R$ (a dimensionless number characterizing the gradients normalized to plasma curvature, which is independent of ρ^*_T as it does not contain the magnetic field intensity), and on the details of the safety factor profile q(r) and magnetic shear *s*.

If the poloidal velocity $V_{\theta i}$ is assumed to be given by neoclassical theory, the corresponding

term in equation (7) scales as the pressure gradient term. Since direct measurements of the poloidal velocity are almost impossible, a neoclassical expression is usually employed to evaluate the poloidal velocity contribution. The neoclassical formula can be reduced to $V_\theta \approx k_{neo} \nabla T_i / (eZ_i B)$, where k_{neo} depends on the collisionality regime. There is no reason for an exact cancellation of the two temperature gradient terms coming from the diamagnetic velocity and from V_θ. The density measurements from Thomson scattering do not allowa reliable estimate of the inverse density gradient length L_n^{-1}. Therefore, for the purpose of our dimensional analysis, we assume L_n^{-1} to be either negligible with respect to L_T^{-1} in evaluating the 'diamagnetic' term, or at most scaling as L_T^{-1} in the ITB region when beam fuelling is significant and particle diffusion is also reduced (this could be justified by the coupling of particle fuelling with the heating source during NBI). Further dependences on L_n/L_T, L_p/L_T, etc., will be assumed to be minor and we shall not consider them explicitly. Then, within a function G_2 of the order of unity, the contributions of the pressure and poloidal velocity to the shear rate scale as

$$\gamma_{E,dia} + \gamma_{E,\theta} = (C_S/L_T)\, \rho_T^* G_2 (s, q, \beta, \nu^*, \ldots) \tag{9}$$

where we have used the same length L_T to dimensionally characterize the maximum gradients inside the ITB and the radial derivative of the pressure gradient which is maximum at the foot of the ITB ($d^2p/dr^2 \approx p/L_T^2$).

Figure 5(a) shows the results of global fluid simulations of 3-D ITG turbulence in the presence of magnetic shear reversal [15]. The q profile was assumed reversed with q_{min} at a rational value (4/3) and then the additional power varied as P_0, $2P_0$, $4P_0$ and $8P_0$ assuming no torque injection, with $T = T_i = T_e$ and $\rho^* = \rho_s/a = 0.01$. The maximum local linear growth rate γ_{max} is first plotted against c_s/L_T. The ratio of the diamagnetic part of the $\boldsymbol{E} \times \boldsymbol{B}$ shear rate $\gamma_{E,\,dia}$ to the dimensionless Larmor radius ρ^*_T is then also plotted against c_s/L_T. All parameters are taken at their maximum values over the radial profile. Both curves illustrate linear dependences and consequently justify the main scalings in our dimensional analysis.

Let us now consider the toroidal velocity contribution. Some experimental observations with strong NBI—typically the case in JET—show the similarity between the ion temperature and toroidal velocity profiles due to comparable heat and momentum diffusivities [16] and to the coupling between the beam heating and the associated torque. We shall then assume, for the sake of simplicity, that the inverse characteristic length over which the toroidal velocity varies is locally comparable with L_T^{-1} (an extra parameter L_ϕ/L_{Ti} could otherwise be introduced in the analysis). In γ_E, the toroidal velocity shear term $\gamma_{E,\,\phi}$ then scales as $M_\phi c_s/L_T$, where M_ϕ is the toroidal flow Mach number, as illustrated in Fig. 5(b), which clearly exhibits the linear dependence of $\gamma_{E,\,\phi}$ on c_s/L_{Ti} for typical experimental examples when the Mach number does not vary substantially.

To summarize, within these approximations, both the diamagnetic and poloidal velocity terms scale as $(c_s/L_T)\rho^*_T$, whereas γ_{max} and $\gamma_{E,\,\phi}$ scale roughly as c_s/L_T. Then simply stating that $\boldsymbol{E} \times \boldsymbol{B}$

stabilization occurs when the terms of order $(c_s/L_T)\rho^*_T$ are large enough, so as to become larger than the combination of the other terms, yields the proposed criterion,

$$\rho^*_T > \rho^*_{ITB}(\Lambda_T, M_\phi, s, q, \beta, \nu^*, \ldots) \tag{10}$$

where ρ^*_{ITB} would in principle depend on a number of dimensionless parameters independent of ρ^*_T such as the q profile, the toroidal Mach number, the β parameter and the collisionality.

The α stabilization [13] can also play an important role in reducing γ_{max} in weak shear discharges. As ρ^*_T, the α parameter increases linearly with $L^{-1}_p \approx L^{-1}_T$, but its local valuewas not found to be constant at the onset of ITBs, and our database analysis did not exhibit a simple and clear correlation between α and the emergence of ITBs.

Although the foregoing interpretation is somewhat heuristic, it is quite remarkable that for the discharges selected, a constant value for ρ^*_{ITB} allows the presence of ITBs to be detected with such a good efficiency despite a variety of plasma scenarios and magnetic field intensities. Strong dependences of ρ^*_{ITB} on some characteristic dimensionless parameters as suggested in equation (10) did not arise for our set of discharges, perhaps because they are not essential, or because the range of variations of these parameters was too limited within this particular database. The lack of a dependence on M_ϕ would imply that diamagnetic and poloidal rotation shears are the main stabilizing terms for the triggering of ITBs. This is probably the case during phases with LHCD only. However, during NBI phases, $\gamma_{E,\,\phi}$ often seems to be the larger component in γ_E if $\gamma_{E,\,\theta}$ is evaluated from neoclassical theory, but this assumption is not quite satisfactory because of the possible existence of so-called self-generated zonal poloidal flows. The proposed interpretation should perhaps stimulate further investigations in which all the anticipated dependences in ρ^*_{ITB} could be varied in a more systematic way, but the fact that ρ^*_{ITB} can be taken as constant for this broad set of data constitutes the major result of the present analysis.

In order to exhibit the bifurcating character of the ρ^*_T stabilization, the physics discussed above can be implemented into a transport coefficient by using a mixing length argument, $\chi_{turb} = \gamma_{eff} L^2_c$, where $\geq eff$ is an effective growth rate ($\geq eff = \geq max$ " $\geq E$) and Lc is the turbulence correlation length. Turbulence simulations show that L_c is proportional to the gyroradius ρ_s in most cases [11, 12, 15] so that the resulting expression for the heat diffusivity is

$$\chi_{turb} = \rho_s C_{sB} F(\Lambda_T, s, \ldots)\, \rho^*_T (\rho_{ITB} - \rho^*_T) \tag{11}$$

where the dimensionless function F measures the stiffness of the model. At large ρ^*_T, the gyro-Bohm scaling of the heat diffusivity is thus weakened—and eventually broken—by the poloidal flow shear stabilization. In non-linear computer simulations [11,15], this breaking is often obtained as the result of increasing $\rho^* = \rho_s/a$ since this parameter is being varied while L_T/R is kept constant. We conjecture that ρ^*_T is indeed the relevant parameter governing this effect, so that reducing locally

the temperature gradient scale length in the plasma through intense heating and at constant magnetic field has a stabilizing effect similar to that of increasing the normalized Larmor radius ($\rho^* = \rho_s/a$) at constant L_T/R in the numerical simulations. A typical set of *S* shaped bifurcation curves can then be obtained by plotting the heat flux as a function of ρ^*_T (Fig.6) since

$$\Gamma_{turb} = nT\, c_s\, F\,(\Lambda_T, s, \ldots)\,(\rho^*_T)^2\,(\rho_{ITB} - \rho^*_T) \tag{12}$$

Therefore increasing the power flux can eventually result in a transition between the gyro-Bohm branch of the curve shown in Fig.6 and the ITB branch. This picture is, of course, simplified because ρ^*_T is not the only parameter which varies and the exact multidimensional dynamics involves other independent parameters (e.g., q, s and β) as well as other transport coefficients (density, momentum). However, in this model the transitionwould start in a region of the plasma where the heat flux corresponds to a local maximum of the flux curve Γ versus ρ^*_T. The increase of ρ^*_T (e.g. due to the powerful heating in optimized shear discharges) can thus be viewed first as the cause of a local bifurcation through diamagnetic turbulence stabilization, but then also as a consequence of the development of the ITB leading to a further increase of ρ^*_T above the critical value until the plasma reaches locally a new equilibrium state (the ITB branch in Fig.6). The critical value, $\rho^*_T = \rho^*_{ITB}$, corresponds to the unstable part of the flux curve and separates a region of turbulent transport where ρ^*_T is strictly below ρ^*_{ITB} and a region of improved confinement where ρ^*_T is strictly larger than ρ^*_{ITB}, i.e. on the stable ITB branch. The spatiotemporal dynamics of such transport bifurcations has been studied theoretically, for instance, in ref. [17].

CONCLUSIONS

In this article, an attempt has been made to identify some simple computable parameters likely to characterize the emergence, location and time evolution of ITBs in JET. Because of the large experimental uncertainties, and sometimes the lack of measurements, a sufficiently reliable calculation of the detailed theoretical expressions describing the growth rates and $\boldsymbol{E} \times \boldsymbol{B}$ shear stabilization of drift waves cannot be routinely performed. Moreover, it would not be suitable for many experimental purposes such as extensive database analysis or real time applications. We have therefore adopted a more pragmatic approach. The simplification of the exact theoretical expressions by means of a dimensional analysis provided a methodology for analysing the data and, at the same time, it yields a plausible physical interpretation of the experimental findings. The simplicity of the resulting criterion fulfils adequately some of the experimental needs (e.g., flexibility of use for real time control and fast computation of ITB characteristics) while it fits the available data fairly well.

Obviously for a given set of fixed dimensional parameters such as the toroidal magnetic field, ion species and plasma temperature, the absolute gradients may seem sufficient to characterize the presence of ITBs. But in the general case where these parameters vary, and when analysing different experimental situations and scenarios, the ratio ρ^*_T of the local ion gyroradius to the local gradient

scale length appears to be the most relevant normalized gradient. It was thus shown that the existence of internal transport barriers in JET can be inferred in regions of space–time where ρ^*_T exceeds some critical value, ρ^*_{ITB}. Dependences of ρ^*_{ITB} on some dimensionless parameters are in principle possible but they are shown not to be essential within this set of experiments. This issue could be further investigated by dedicated experiments on JET or on other machines. Thus, at this stage, the correlation between the emergence of ITBs and the criterion $\rho^*_T > \rho^*_{ITB}$ with constant ρ^*_{ITB} may not be sufficiently general to be applied for predictive purposes in all circumstances and all devices. Nevertheless, it has been successfully tested on a wide variety of JET discharges. The examination of the contour graphs in addition to the statistics collected from 116 discharges demonstrates the relevance and usefulness of ρ^*_T in characterizing the appearance of ITBs, at least empirically. Applying the criterion to this set of discharges yielded only 5% of the detection errors, with an ITB emergence time uncertainty of the order of 150ms and an error of location of 4.7cm with respect to the figures obtained by an independent and tedious shot by shot data analysis.

The proposed ρ^*_T criterion allows the detection and localization of ITBs under various experimental conditions, and provides convenient displays of their evolution. It accounts for the measurement uncertainties, can be applied to the electron or ion temperature profiles and is practical to use for the systematic analysis of experimental data and the handling of large databases [18]. Finally, it can be obtained at low computational cost. Thus, it may also find a number of applications in the operation of tokamak devices, such as the real time control of ITBs which has been recently implemented on JET [18, 19] and which should constitute a significant step towards the development of advanced tokamak steady state operation scenarios.

ACKNOWLEDGMENTS

This work was performed under the auspices of the European Fusion Development Agreement. Particular thanks are due to A. Bécoulet for his encouragement, E. Joffrin for his help in data analysis and P. Maget for fruitful discussions.

REFERENCES

[1]. Taylor T.S. 1997 *Plasma Phys. Control. Fusion* **39** B47 and references therein
[2]. Gormezano C. 1999 *Plasma Phys. Control. Fusion* **41** B367
[3]. Sakamoto Y. *et al* 2001 *Nucl. Fusion* **41** 865
[4]. Connor J.W. and Wilson H.R. 1994 *Plasma Phys. Control. Fusion* **36** 719
[5]. Horton W. 1999 *Rev. Mod. Phys.* **71** 735
[6]. Christiansen J.P. *et al* 1993 *Nucl. Fusion* **33** 863
[7]. Challis C. *et al* 2001 *Plasma Phys. Control. Fusion* **43** 861
[8]. Dorland W. and Hammett G.W. 1993 *Phys. Fluids* B **5** 812
[9]. Waltz R.E., Kerbel G.D. and Milovitch J. 1994 *Phys. Plasmas* **1** 2229
[10]. Waltz R.E. *et al* 1995 *Phys. Plasmas* **2** 2408

[11]. Garbet X. and Waltz R.E. 1996 *Phys. Plasmas* **3** 1898
[12]. Manfredi G. and Ottaviani M. 1997 *Phys. Rev. Lett.* **79** 4190
[13]. Beer M.A. *et al* 1997 *Phys. Plasmas* **4** 1792
[14]. Burrell K.H. 1997 *Phys. Plasmas* **4** 1499
[15]. Garbet X. *et al* 2001 *Phys. Plasmas* **8** 2793
[16]. de Esch H.P.L. *et al* 1990 *Proc. 17th Eur. Conf. on Control. Fusion and Plasma Heating (Amsterdam, 1990)* vol 14B, part I (Geneva: European Physical Society) 90
[17]. Lebedev V.B. and Diamond P.H. 1997 *Phys. Plasmas* **4** 1087
[18]. Tresset G. *et al* 2001 *Proc. 28th Eur. Conf. on Control. Fusion and Plasma Physics (Madeira, 2001)* vol 25A (Geneva: European Physical Society) CD-ROM
[19]. Mazon D. *et al* 2001 *Proc. 28th Eur. Conf. on Control. Fusion and Plasma Physics (Madeira, 2001)* vol 25A (Geneva: European Physical Society) CD-ROM

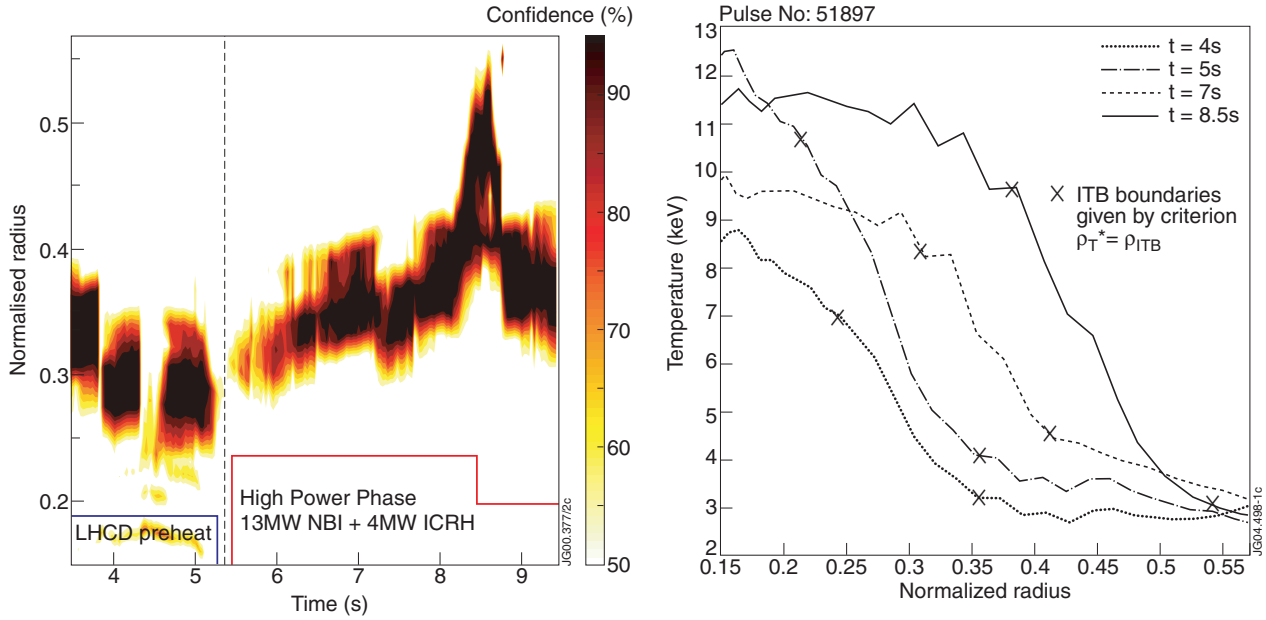

Figure 1: (a) Constant-$\wp_{ITB}$ contours plotted for $\wp_{ITB}(R, t) \geq 50\%$ showing the space–time evolution of an electron ITB (Pulse No: 51897). (b) Profiles of electron temperature at 4, 5, 7 and 8.5s from ECE. The crosses symbolize the boundaries of the barrier as inferred from the criterion $\rho^*_T = \rho^*_{ITB}$ (Pulse No: 51897).

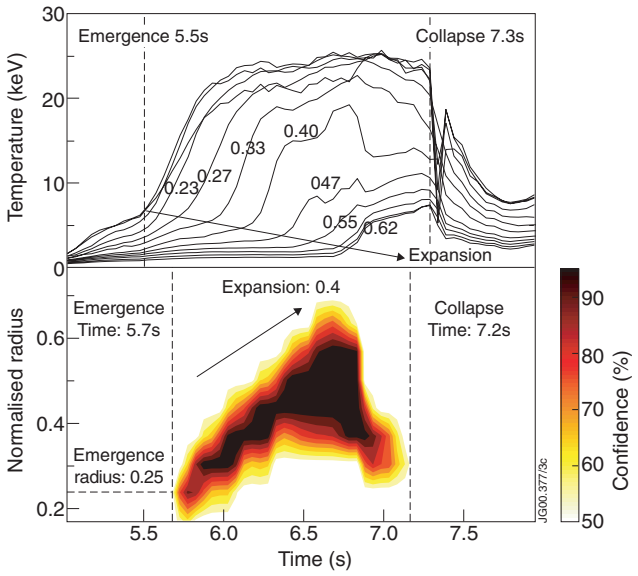

Figure 2: Top frame: time evolution of the ion temperature at various normalized radii (Pulse No: 40030). Bottom frame: constant-$\wp_{ITB}$ contours.

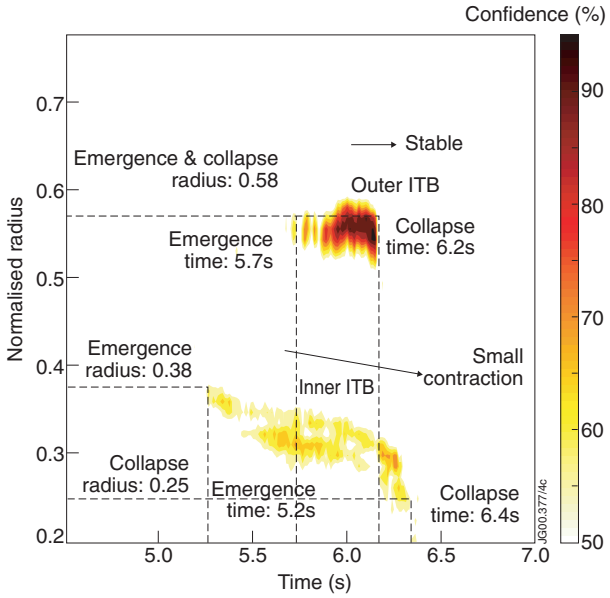

Figure 3: Constant-$\wp_{ITB}$ contours showing two ITBs on the electron temperature profiles (Pulse No: 49680).

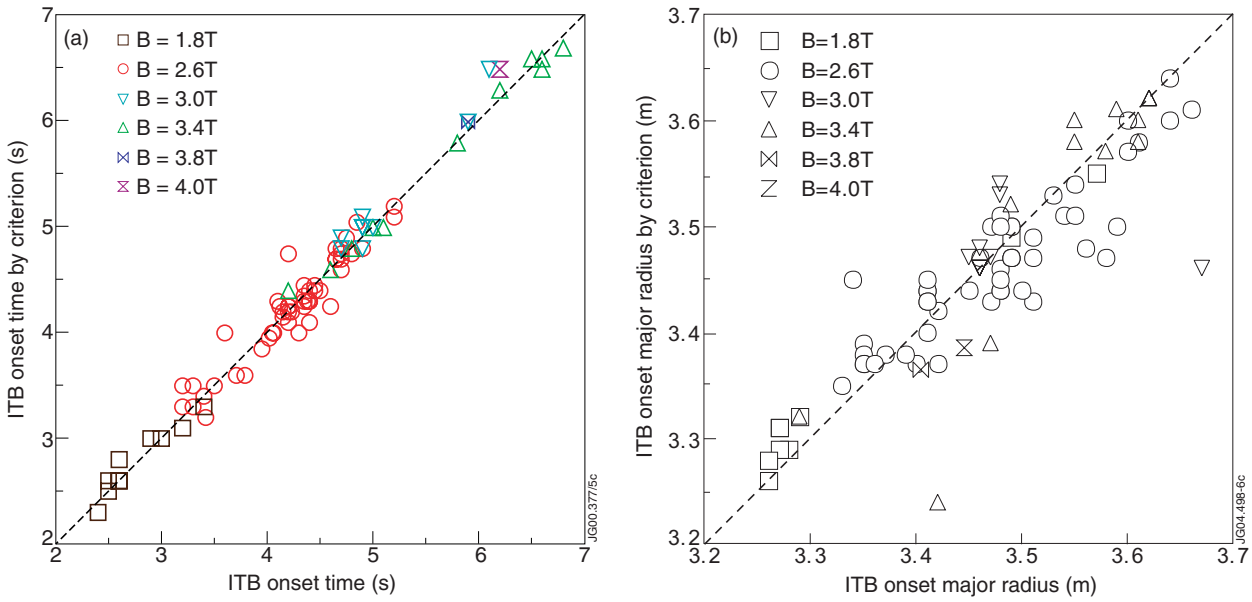

Figure 4: (a) Statistics on the validation of the ITB emergence time through the ρ^*_T criterion for various magnetic field intensities. The emergence time determined by $\rho^*_T = \rho^*_{ITB}$ is plotted against that determined independently from data analysis. (b) Same as (a) for the ITB emergence major radius. The emergence radius determined by $\rho^*_T = \rho^*_{ITB}$ is plotted against that determined independently from data analysis.

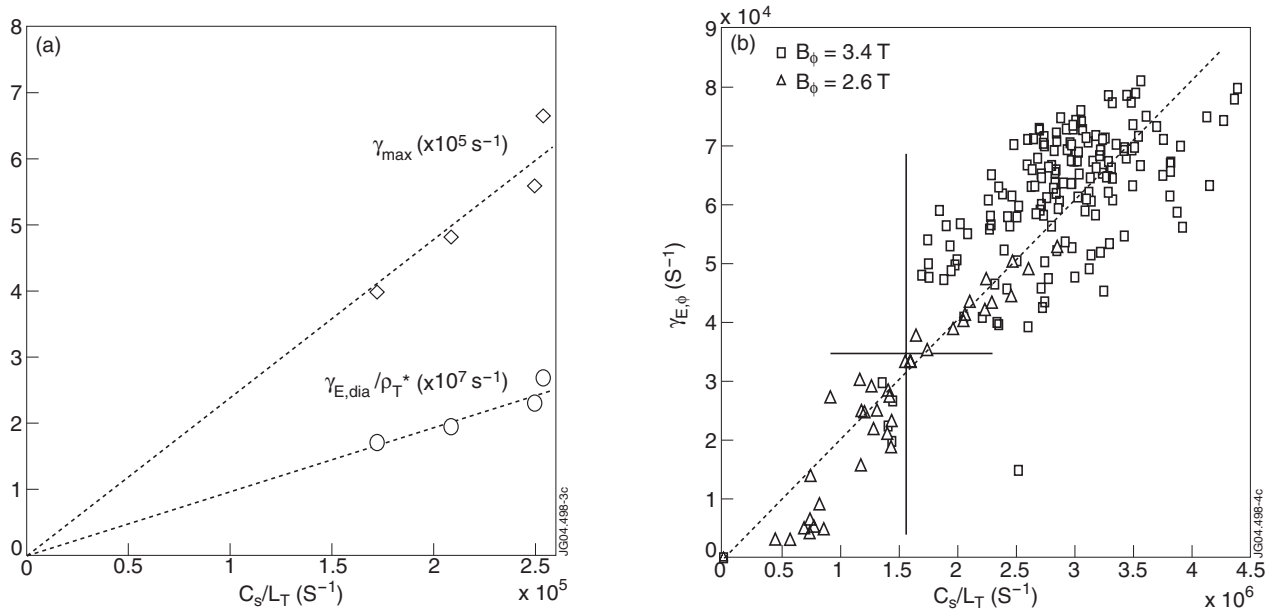

Figure 5: (a) Maximum linear growth rate γ_{max} versus c_s/L_T (diamonds) and ratio of the diamagnetic part of the E $\times$B shear rate $\gamma_{E,\,dia}$ to the dimensionless Larmor radius ρ^*_T versus c_s/L_T (circles). The results are shown of global fluid simulations of 3-D ITG turbulence in the presence of magnetic shear reversal [15] with four different additional powers and no torque injection. Here $T = T_i = T_e$ and $\rho^* = 0.01$. All the data are taken at their maximum values over the radial profile. (b) Toroidal velocity term in the E $\times$B shear rate $\gamma_{E,\,\phi}$ versus c_s/L_{Ti} for two JET discharges at B_ϕ = 3.4T (squares, Pulse No: 53521) and B_ϕ = 2.6T (triangles, Pulse No: 49645). The data are averaged over the radial profile and plotted at various times.

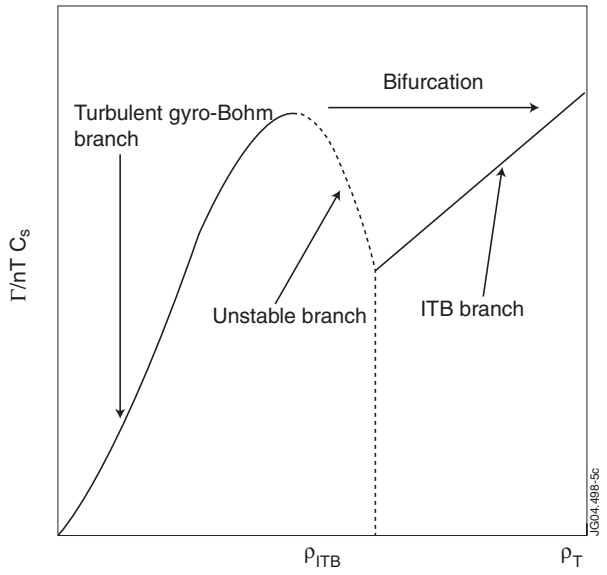

Figure 6: Normalized heat flux versus ρ^*_T, showing the multivaluedness of ρ^*_T, and the possible bifurcation from turbulent gyro-Bohm transport to the ITB branch.